Robust Shape Recovery for Sparse Contact Location and Normal Data from Haptic Exploration

A. Bierbaum, I. Gubarev and R. Dillmann
Institute of Computer Science and Engineering
University of Karlsruhe (TH)
Karlsruhe, Germany
{bierbaum,dillmann}@ira.uka.de

***Abstract*— 3D shape reconstruction of objects from tactile exploration data acquired by a multi-fingered robot hand is an important skill for a humanoid robot system. Tactile exploration data captured using current robot technology is naturally sparse and noisy, therefore a satisfying shape estimate is difficult to achieve. In this paper we describe a robust approach for 3D shape recovery using superquadric functions, which makes use of both contact location and normal information. We present two quality measures and compare to other relevant estimation techniques using representative synthetic contact data.**

I. Introduction

Active touch exploration enables human not only to perceive local physical object features as texture or rigidity but also to sense the exact shape of an object. This sensual input is a supplement to the information given by visual perception and stabilizes our internal spatial representation of a real world object. The integration of haptic sensing has become an important issue in the field of humanoid robotics and may be used to complement the pre-dominant sense of vision in 3D shape reconstruction of unknown or partially known objects.

A volumetric object model constructed from haptic exploration data delivers a rather high amount of information for discriminating between objects. Also, volumetric object data is most suitable for supplementing and verifying geometric information in multimodal object representations. The concept of superquadrics has been introduced in [1] as a family of parametric 3D shapes, among which the superellipsoid has become the most popular one and is often termed as superquadric, a convention we will preserve here. By applying estimation techniques, basic 3D point clouds from cubic or spheric bodies may be represented as superquadrics. To represent more complex shapes, segmentation and decomposition methods for point clouds have been presented, e.g. in [2]. Only recently this algorithm has been applied in the context of grasp planning for complex 3D objects in [3].

Several approaches have been proposed for acquiring and modeling object shape information by robots through haptic exploration. An early, comprising experimental setup was presented in [4]. Here a dextrous robot hand probed contact on test objects at predefined positions. The resulting sparse point clouds were fitted to superquadric models. In addition to the contact locations, the contact normal information was used in [5], [6] to construct a polyhedral 3D model from contact exploration data.

In [7] we have presented a framework for haptic exploration for both, a human hand wearing a data glove with finger tip contact sensors and a humanoid robot hand. The resulting 3D point clouds were fitted to superquadric models. When using only contact location data, the quality of the fit appeared quite depending on the distribution of the acquired data points. A comprehensive haptic exploration process was required to collect a number of sample points which were sufficient to give good correspondence between real world object and estimate. In order to improve robustness and reduce the number of required data points, we decided to integrate available contact normal information and use an enhanced estimation scheme.

Here, we present our results from investigation and evaluation of a hybrid estimation technique using a *genetic algorithm* (GA) which was originally developed in the context of range imaging. For applying the algorithm we created representative synthetic data sets from a virtual haptic exploration process, as it could be expected when using tactile and proprioceptive sensors on a multi-fingered robot hand. For comparison of the results we also developed specific measures of quality. The development of a dexterous exploration strategy itself is not part of this work. Yet, this issue has received very limited amount in literature, some preliminary work may be found in [8], [6].

This paper is organized as follows. In the next section the relevant details and properties of superquadric functions are described alon with applicable estimation techniques for 3D point clouds. In Section III we present the generation of synthetic contact data from a virtual haptic exploration procedure and define a measure of quality for evaluation of the algorithms. Further, we show our results by comparing the performance of standard and hybrid algorithms applied to contact data with and without normal information. Finally we give a conclusion and an outlook on our future work in Section V.

II. Superquadric Estimation Techniques

A. Definition of Superquadrics

A superquadric centered in the origin and with its axes aligned to the x, y, z coordinate axes can be described with

the following parametric equation

$$\chi(\eta,\omega) = \begin{pmatrix} a_1\ \cos^{\varepsilon_1}(\eta)\ \cos^{\varepsilon_2}(\omega) \\ a_2\ \cos^{\varepsilon_1}(\eta)\ \sin^{\varepsilon_2}(\omega) \\ a_3\ \sin^{\varepsilon_1}(\eta) \end{pmatrix} \quad . \tag{1}$$

The parameter vector $\mathbf{a} = (a_1, a_2, a_3)^T$ describes the extent of the superquadric along each axis. The exponents ε_1, $\varepsilon_2 \in [0..2]$ produce a variety of convex shapes and describe the shaping characteristics from cubic to round in x and y directions. This way different 3D primitive shapes can be modeled, e.g. boxes ($\varepsilon_1, \varepsilon_2 \approx 0$), cylinders ($\varepsilon_1 = 1, \varepsilon_2 \approx 0$) and ellipsoids ($\varepsilon_1, \varepsilon_2 = 1$).

To locate the superquadric arbitrarily in space, we further introduce a rotational matrix $\mathbf{R}$ and a translation $\mathbf{x_0}$, which add 6 more parameters to our model.

As superellipsoids are restricted to symmetric shapes only, we add deformation parameters $\{t_x, t_y \in [-1..1]\}$ for modeling tapering in z direction as described in [9]. This enables our model to also represent wedge resembling shapes. Applying a scaled tapering deformation function

$$D_t(x,y,z) = \begin{pmatrix} t_x \frac{z}{a_3} + 1 \\ t_y \frac{z}{a_3} + 1 \\ 1 \end{pmatrix} \begin{pmatrix} x \\ y \\ z \end{pmatrix} \tag{2}$$

we finally get the model function

$$\mathbf{x} = \mathbf{R} D_t(\chi(\eta,\omega)) + \mathbf{x_0} \quad .$$

The normal vectors of the surface of a superquadric may be computed via cross product as

$$\mathbf{n}(\eta,\omega) = \frac{\partial \chi}{\partial \eta} \times \frac{\partial \chi}{\partial \omega} \quad . \tag{3}$$

Applying any superquadric global deformation to the normal vector results in

$$\mathbf{n_d} = \det J\ J^{-1T}\ \mathbf{n} \quad , \tag{4}$$

where J is the Jacobian matrix of the deformation [10]. For the final vectors we use the rotation matrix in global space

$$\mathbf{N} = \mathbf{R} \det J_t\ J_t^{-1T}\ \mathbf{n} \quad , \tag{5}$$

where J_t is a Jacobian matrix for tapering deformation defined in eq. (2).

By rendering a superquadric according to eq. (1), we emphasize regions exhibiting high curvature (fig. 1). For an unbiased sample distribution we need to apply equidistant rendering using spherical angles as introduced by Bardinet [11],

$$\chi'(\eta,\omega) = \begin{pmatrix} a_1\ \rho\ \cos(\eta)\ \cos(\omega) \\ a_2\ \rho\ \cos(\eta)\ \sin(\omega) \\ a_3\ \rho\ \sin(\eta) \end{pmatrix} \quad , \tag{6}$$

where

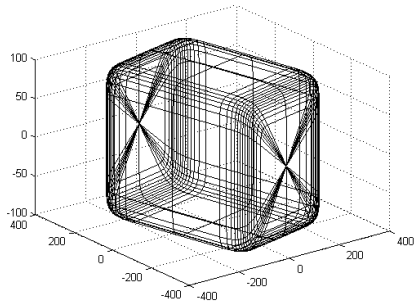

(a) Natural parametrization

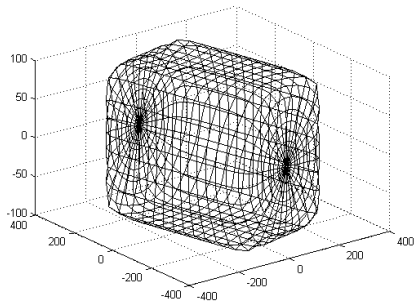

(b) Uniform parametrization

Fig. 1. Superquadric parametrizations

$$\rho = \left(\left(|\cos\omega\cos\eta|^{\frac{2}{\varepsilon_2}} + |\sin\omega\cos\eta|^{\frac{2}{\varepsilon_2}} \right)^{\frac{\varepsilon_2}{\varepsilon_1}} + |\sin(\eta)|^{\frac{2}{\varepsilon_1}} \right)^{\frac{-\varepsilon_1}{2}} \quad .$$

Applying (3) and (6) we may compute normal vectors using uniform parametrization.

B. Superquadric estimation

To estimate superquadric parameters from a given 3D point set with additional normal information we need to define an error-of-fit (EOF) measure and search the global minimum of this function in the valid parameter domain. Search starts around an initial estimate $\chi(\eta,\omega)_E$ which is computed as follows. The initial translation $\mathbf{x_0}_{,E}$ is calculated as centroid of the dataset. The elements of the extension parameter vector $\mathbf{a}_E$ are set to the maximum extension along each axis respectively. The rotational matrix $\mathbf{R}_E$ is initialized with the principal axes as eigenvectors of the covariance matrix of the data set, see [9] for details. Curvature parameters are initially set to $\varepsilon_{1,E} = \varepsilon_{2,E} = 1$, thus describing an ellipsoid.

We use metrics based on radial Euclidian distance (fig. 2), combining distance from sample coordinates to the superquadric surface and distance between given and estimated surface normal vectors. For contact points we use a distance metric Boult and Gross [12] suggested

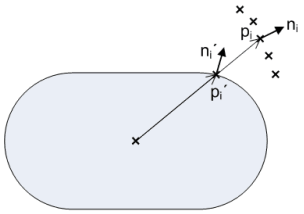

Fig. 2. Coordinate and normal vectors for original primitive and estimate.

$$D_i^{(1)} = \|\mathbf{p_i}\| \left(1 - \frac{1}{F(\mathbf{p_i})}\right), \tag{7}$$

where $F(\mathbf{p_i})$ is the inside-outside function of the superquadric [9]. For surface orientation vector distance we compute

$$D_i^{(2)} = \left\| \frac{\mathbf{n_i}}{\|\mathbf{n_i}\|} - \frac{\mathbf{n_i'}}{\|\mathbf{n_i'}\|} \right\|^2 \tag{8}$$

for each input normal vector $\mathbf{n_i}$ and corresponding surface orientation $\mathbf{n_i'}$. The final EOF is defined as

$$D = \frac{1}{p} \sum_{i=1}^{p} \left(\left| D_i^{(1)} \right| + \lambda \sigma D_i^{(2)} \right)^2 \tag{9}$$

for p contact points with normal information, where $\sigma = (a_1 + a + a_3)/3$ is a normalizing factor adjusting the vector distance to the size of the superquadric and λ is a weighting factor for surface orientation in the final error function [13].

Many superquadric recovery approaches [9], [11] use nonlinear least-squares minimization (NLLSM) techniques to find parameters for best approximation of a point cloud [14]. In general these methods are afflicted with the problem of terminating in a *local* minimum in the parameter space around the initial estimate. By adding a surface orientation component to the EOF we increase the number of local minima, also in the immediate neighbourhood of the global minimum. Some studies used simulated annealing to overcome the locality problem of the NLLSM [13], [15]. Also, this method requires a good initial estimate to converge to the optimum solution.

In case of sparse data the number of local minima increases and even more scatters throughout parameter space. The quality of the initial guess is not equally guaranteed. It is often required to rotate and resize a considerable amount from the intial estimate to approach the global minimum. Working on sparse and noisy data as exhibited by contact data from haptic exploration the estimation method has to overcome flat *and* deep local minima. In our experiments we used a genetic algorithm (GA) in a hybrid approach, first introduced in [16], as a combination of GA with NLLSM.

C. Genetic Algorithms for superquadric estimation

A GA explores several regions of parameter space simultaneously. The iterative process *evolves* a population of possible solutions according to Darwinian theory of evolution. A GA is characterized by

- an encoding of a possible solution, so called *chromosome*,
- a *population pool* of chromosomes,
- a *fitness function* for *parent selection*,
- and chromosome *reproduction* applying several *genetic operations*.

The chromosomes of the actual population pool are evaluated during each iteration step. The parents for reproduction are randomly selected, prefering the individuals with highest fitness. In a next step genetic operations are randomly applied to parents to compute the population pool . The two most common operations are *mutation* and *crossover*. Mutation randomly changes a part of the chromosome while crossover randomly combines elements of parents' chromosomes.

For superquadric fitting we represent a vector of parameters (a, ϵ, t, R, x_0) by a chromosome. For computing fitness we use the EOF function as defined in eq. (9).

A clear disadvantage in using GA is the low convergence speed. Once the algorithm finds the parameter space containing the global minimum, the next goal is to converge to the global minimum within this space. Aborting GA at this state and using the intermediate solution as the initial estimate of the NLLSM algorithm provides faster convergence. This combination is called a *hybrid approach*.
The major difficulty is to find an abortion criterium of the GA part which trades off between accuracy and convergence speed. In general, GA may be aborted at a small residual value, on time expiration or after a defined generation count has passed.

III. Algorithm Evaluation

A. Generation of Synthetic Data

To abstract from physical sensor data we investigated the performance of different EOF functions and minimization algorithms applied to synthetic haptic exploration data. We use convex primitives as objects which may be represented as single tapered superquadrics. Other approaches [11], [12], [13], [16], [9], [15] used multiview range images as input data for the estimator.

To simulate realistic input data from haptic exploration with a multi-fingered robot hand we generate sparse contact data patterns of two types:

1) A *stripe* is represented as a single line in the (η, ω) space, which is initially rendered for n points. These points in the (η, ω) space are then rendered equidistant to the contact points in the Euclidian space and the corresponding normal vectors (eq. 6). A stripe represents the exploration path of a single finger tip of a robot hand as it results from a contour following task, see also [17].
2) A *randomized patch* is represented by a rectangular region in the (η, ω) space. We randomly select n points from this region and perform uniform rendering to the contact points with corresponding normal vectors. Such a randomly sampled region represents data from a locally bounded exploration process, as it results from a local contact of a finger tip sensor on the object.

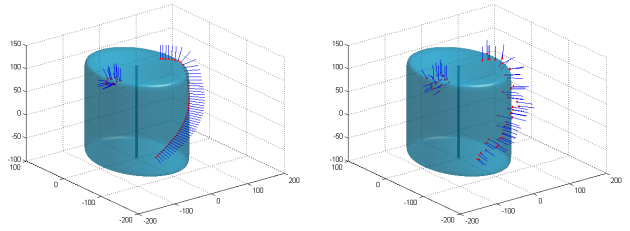

(a) Unbiased contact data (b) Contact data with 10% gaussian noise

Fig. 3. Examples of the exploration patterns *stripe* and *patch* with point and normal information.

For modelling the contact data from a haptic exploration procedure we choose a combination of different data patches and stripes at distinct locations and along different trajectories and merge these to an exploration dataset. The datasets are created manually with the goal to emulate real contact traces of the finger tips of an exploring dexterous robot hand equipped with finger tip tactile sensors. The composition process is empirically, following oberservations of data patterns as seen with our exploration framework [7]. Natural haptic exploration is always of a local nature therefore we kept the composed data sparse, as it might result from a short exploration procedure following an initial contact. We do not consider temporal characteristics, i.e. incremental emergence of the data, but create a static data set. Consistently, we assume the pose of the shape to be fixed and the object to be stationary throughout generation of exploration patterns.
To emulate measurement inaccuracy we finally add Gaussian noise to both contact point coordinates *and* normal vector components (fig. 3).

B. Quality measures

Evaluation of different algorithms requires comparative metrics for estimated superquadrics. Direct comparison of superquadric parameters with those of the original primitive is not representative due to ambiguities in the superquadric representation [9]. The application of weighting factors for different parameters in the final rating is complex due to different units of measure. Using the final EOF as metric is also vague due to random noise.

We use the following two metrics for algorithm evaluation:

- To determine the minimization quality of the algorithm we define

$$\vartheta = \frac{D(S_e)}{D(S_s)+1}, \tag{10}$$

where D is the EOF defined in (9) and S_e, S_s are the estimated and synthetic superquadrics (for contact points only we can define $\vartheta^{(1)}$ over $D^{(1)}$). Presuming that the global minimum EOF is less than $D(S_s)$, $\vartheta > 1$ means that the parameters of the estimated superquadric do not minimize the EOF function to the optimum. Further, $\vartheta \ll 1$ implies that the synthetic object is far from the global minimum described by the 3D point set, so the input data is not representative. In this case we need more contact points with normal information for sufficient estimation of shape and pose parameters.

- The second quality measure is based on the volume of the intersection of estimated and synthetic superquadrics. We define α-error or *false positives* as

$$\alpha = \frac{V(\{p | p \in S_e \wedge p \notin S_s\})}{V(S_e)}, \tag{11}$$

and β-error or *false negatives* as

$$\beta = \frac{V(\{p | p \in S_s \wedge p \notin S_e\})}{V(S_s)}. \tag{12}$$

V represents the volume of a superquadric or part of a superquadric. The weighting factor of the α- and β-errors in the final evaluation is scenario specific. We used $\epsilon = \alpha + \beta$ as the second quality measure in our experiments.

IV. Simulation Results

We evaluated four schemes for the estimation of superquadric functions from synthetic exploration data:

1) Contact location information with NLLSM (LS).
2) Contact location information with hybrid minimization (H).
3) Contact location and normal information with NLLSM (nLS).
4) Contact location and normal information with hybrid minimization (nH).

In all experiments we used $\lambda = 0.5$ in eq. (9). The standard deviation σ_N of the generated noise was set to 10% of the nominal value.
Results are shown in figure 4. The column pictures show (a) original primitive and data samples, (b) LS fit, (c) H fit, (d) nLS fit, (e) nH fit. The resulting estimated superquadrics are coloured orange and superimposed to the original primitive in blue.
The synthetic data sets comprised 150 contact points and corresponding normal vectors for each body investigated. The locations for patch and stripe contact data patterns were selected empirically in a way that reconstruction with the given superquadric model must be distinct. For prismatic shapes we added data from patch exploration at a corner region of the respective object, covering all adjacent faces. This way the tapering function D_t is disambiguated. Further, we added one or more stripe patterns crossing edges and adjacent faces so that extension **a** and shape parameters ε_1,ε_2 may be estimated. As the ellipsoid body does not have edges we applied only patch contact patterns here, like they may result from contact probing with thumb and index. In general, the applied contact pattern sets aimed to imitate simple, short term exploratory procedures of a multi-fingered hand with few reconfiguration steps. E.g. one could imagine a thumb touching the cubes corner while moving three fingers in parallel across its side face.

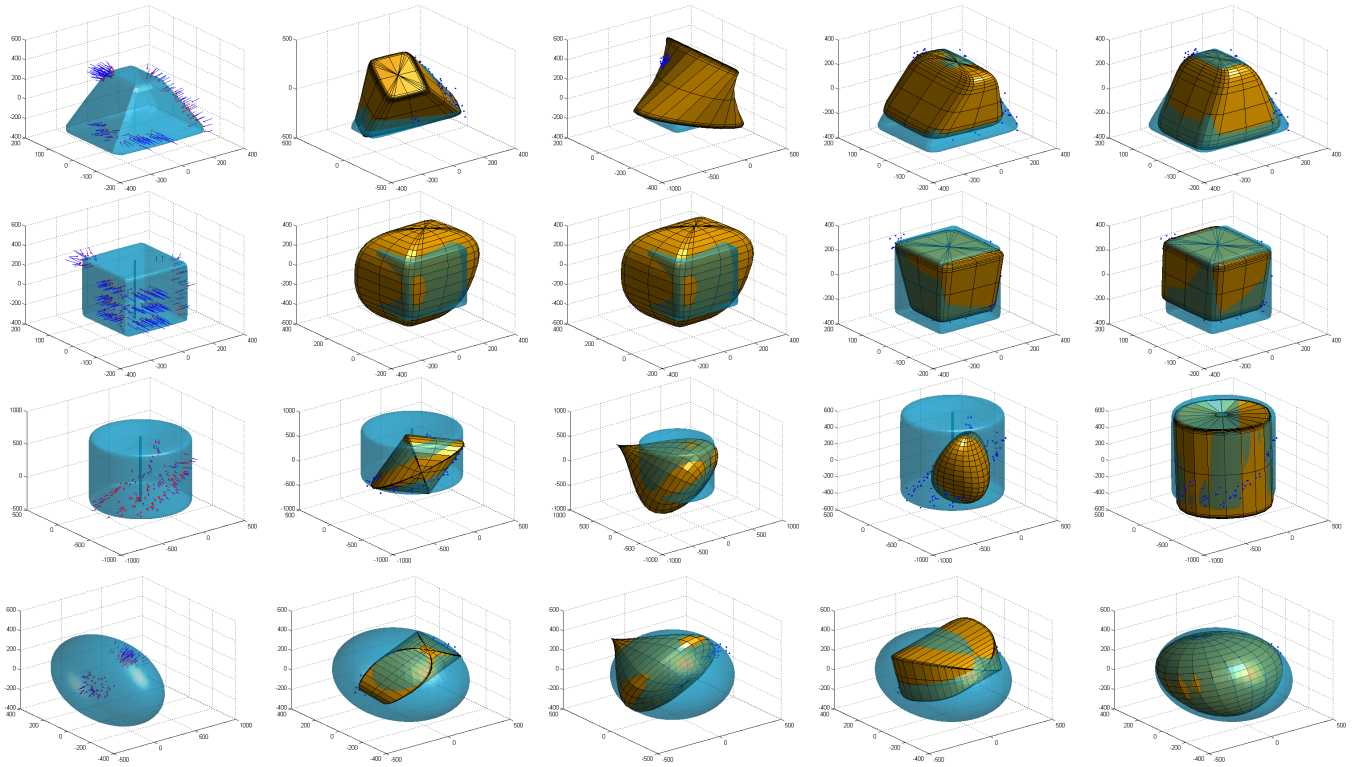

(a) (b) (c) (d) (e)

Fig. 4. Fitting results from top to bottom: Tapered Box, Cube, Cylinder, Ellipsoid. Columns show (a) original primitive and data samples, (b) LS fit, (c) H fit, (d) nLS fit, (e) nH fit. Resulting fits are coloured orange and superimposed to the original primitive (blue).

A question which may arise is how the quality of the fit with the method proposed would change with different synthetic data sets as input. Basically, the data must support the shape features in a distinct way to achieve non-ambiguous results, which is a characteristic we provided in case of our synthetic exploratio data, as stated above. Otherwise the fitting process may result in an estimate not corresponding to the true shape. For an autonomous system, the optimal selection of contact regions should be assigned to the exploration strategy, which is not part of this work.

By sight, our hybrid approach using both contact location and normal information provides the best shape estimates for the data. It can be said that the inclusion of contact normal data seems to improve the results for the mere LS based method, but not to the same degree as with the hybrid variant. This is related to GA's capability of surmounting local minima while searching the global minimum. Note that due to our implementation NLLSM performs an average of 20 evaluations for descending per iteration step, while the hybrid method requires 100 evaluations per iteration to calculate the next generation. The evaluation count was limited to the same number for all schemes to allow comparison. In our implementation running on a Pentium IV (3.0 GHz, 1Gb RAM) processing time was 500 to 1000 evaluations per second, depending on load.

Finally we investigated the performance of the algorithms with different time limitations and noise levels as shown in figure 5. In case of the hybrid approach, results from 10 estimation runs were averaged, as the GA method introduces random operations. For comparing quality vs. n a cylinder primitive was subject to estimation, while for quality vs. σ_N a cube primitive was chosen. Note that exploration sample data noise is regenerated randomly each estimation run.

As can be seen, the volume coverage measure ϵ indicates slow and unstable characteristics for NLLSM with increasing number of evaluations, while the hybrid algorithms converge more stable and towards adequate minimal values for both criteria. With increasing noise level the inclusion of contact normal data stabilizes the estimation results for both LS and hybrid estimation, but here also the hybrid approach shows to be superior in terms of robustness and quality of fit.

V. Conclusions

In this paper we presented a method for estimating superquadric shape representations from sparse and noisy contact normal and location data as acquired by haptic exploration with multi-fingered robot hands using finger tip tactile sensors. By considering the contact normal information and applying a hybrid minimization method utilizing a genetic algorithm, we could recover superquadric primitives in a robust and stable manner from synthetic exploration data. We developed two meaningful measures of quality and compared our method with the standard least-squares estimation technique and with a hybrid approach involving contact point locations only.

Concerning our evaluation we state that more realistic ex-

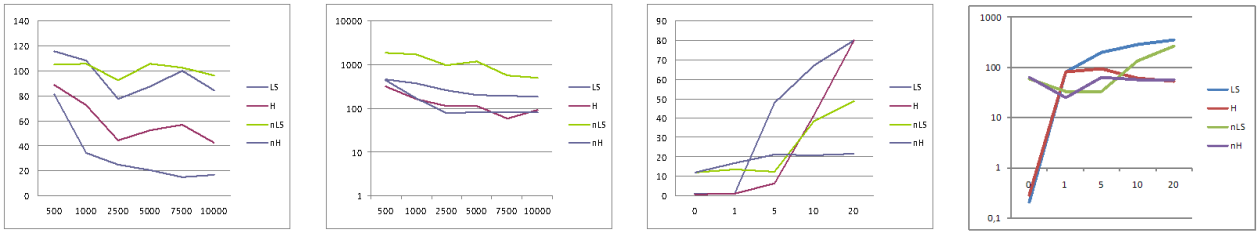

(a) ϵ-error % vs. n (b) ϑ, $\vartheta^{(1)}$ in % vs. n (c) ϵ-error in % vs. σ_N (d) ϑ, $\vartheta^{(1)}$ vs. % σ_N

Fig. 5. Quality vs. evaluation count n and standard deviation σ_N of the noise level. The latter is plotted in logarithmic scaling.

ploration data could be created by using a more detailed simulation of the exploration process, which is work in progress. This also involves development of autonomous and robust haptic exploration strategies for the robot hand. Yet, we feel the synthetic exploration data used in the work presented is more detailed than in previous studies [8], [6]. A basic disadvantage in using a GA for estimation is the higher amount of computing time compared to NLLSM, but in our view the superior performance of this method justifies its application here. Further, we expect this to become a minor problem when transferring the method to hardware suited for parallel computing.

As a next step we will move to the acquisition of real world exploration data by our humanoid robot, which has two five-finger hands equipped with tactile sensors [18], and investigate the performance of the developed estimation technique with this data. For haptic exploration of complex objects we further plan to integrate decomposition methods in our estimation scheme which provide the separation of complex 3D structures into superquadric primitives.

Acknowledgement

The work described in this paper was conducted within the EU Cognitive Systems project PACO-PLUS (FP6-2004-IST-4-027657) funded by the European Commission.

References

[1] A.H. Barr, "Superquadrics and angle-preserving transformations," *Computer Graphics and Applications, IEEE*, vol. 1, no. 1, pp. 11–23, Jan 1981.

[2] L. Chevalier and F. Jaillet, "Segmentation and superquadric modeling of 3d objects," in *Proceedings of WSCG*, 2003.

[3] Corey Goldfeder, Peter K. Allen, Claire Lackner, and Raphael Pelossof, "Grasp planning via decomposition trees," in *Robotics and Automation, 2007 IEEE International Conference on*, 10-14 April 2007, pp. 4679–4684.

[4] P.K. Allen and K.S. Roberts, "Haptic object recognition using a multi-fingered dextrous hand," in *Robotics and Automation, 1989. Proceedings., 1989 IEEE International Conference on*, 14-19 May 1989, vol. 1, pp. 342–347.

[5] S. Caselli, C. Magnanini, and F. Zanichelli, "Haptic object recognition with a dextrous hand based on volumetric shape representations," in *Multisensor Fusion and Integration for Intelligent Systems, 1994. IEEE International Conference on MFI '94.*, 2-5 Oct. 1994, pp. 280–287.

[6] S. Caselli, C. Magnanini, F. Zanichelli, and E. Caraffi, "Efficient exploration and recognition of convex objects based on haptic perception," in *Robotics and Automation, 1996. Proceedings., 1996 IEEE International Conference on*, 22-28 April 1996, pp. 3508 – 3513 vol.4.

[7] A. Bierbaum, K. Welke, D. Burger, T. Asfour, and R. Dillmann, "Haptic exploration for 3d shape reconstruction using five-finger hands," in *Proc. IEEE-RAS International Conference on Humanoid robots*, Pittsburgh PA, USA, Nov 29 - Dec 01 2007.

[8] K.S. Roberts, "Robot active touch exploration: constraints and strategies," in *Robotics and Automation, 1990. Proceedings., 1990 IEEE International Conference on*, 13-18 May 1990, pp. 980–985 vol.2.

[9] F. Solina and R. Bajcsy, "Recovery of parametric models from range images: the case for superquadrics with global deformations," *Pattern Analysis and Machine Intelligence, IEEE Transactions on*, vol. 12, no. 2, pp. 131–147, Feb. 1990.

[10] Barr, "Global and local deformations of solid primitives," *ACM SIGGRAPH Computer Graphics*, vol. 18, pp. 21–30, 1984.

[11] Eric Bardinet, Laurent D. Cohen, and Nicholas Ayache, "A parametric deformable model to fit unstructured 3D data," *Computer Vision and Image Understanding: CVIU*, vol. 71, no. 1, pp. 39–54, 1998.

[12] A.D. Gross and T.E. Boult, "Error of fit measures for recovering parametric solids," in *Computer Vision., 1988. Second International Conference on*, December 5-8, 1988, pp. 690–694.

[13] Kenong Wu and M.D. Levine, "Recovering parametric geons from multiview range data," in *Computer Vision and Pattern Recognition,IEEE Computer Society Conference on*, June 1994, pp. 159–166.

[14] Donald W. Marquardt, "An algorithm for least-squares estimation of nonlinear parameters," *SIAM Journal on Applied Mathematics*, vol. 11, no. 2, pp. 431–441, 1963.

[15] N. Yokoya, M. Kaneta, and K. Yamamoto, "Recovery of superquadric primitives from a range image using simulated annealing," in *Pattern Recognition, 1992 . Vol.1. Conference A: Computer Vision and Applications, Proceedings., 11th IAPR International Conference on*, 30 Aug.-3 Sept. 1992, pp. 168–172.

[16] J. Sinnott and T. Howard, "A hybrid approach to the recovery of deformable superquadric models from 3d data," in *Proc. Computer Graphics International*, 2001, pp. 131–138.

[17] N. Chen, R. Rink, and H. Zhang, "Local object shape from tactile sensing," in *Robotics and Automation, 1996. Proceedings., 1996 IEEE International Conference on*, 22-28 April 1996, vol. 4, pp. 3496–3501vol.4.

[18] T. Asfour, K. Regenstein, P. Azad, J. Schroder, A. Bierbaum, N. Vahrenkamp, and R. Dillmann, "Armar-iii: An integrated humanoid platform for sensory-motor control," in *Humanoid Robots, 2006 6th IEEE-RAS International Conference on*, Dec. 2006, pp. 169–175.